Dual-Function Electroabsorption Waveguide Modulator/Detector for Optoelectronic Transceiver Applications

R. B. Welstand, S. A. Pappert, C. K. Sun, J. T. Zhu, Y. Z. Liu, and P. K. L. Yu, *Member, IEEE*

***Abstract*— A Franz–Keldysh effect InGaAsP electroabsorption waveguide device is utilized as a high-frequency, high-linear dynamic range modulator and photodetector. The dual-function modulator/photodetector can be useful in compact transmit/receive front end antenna architectures. Adjusting the electrical bias to the reverse-biased p-i-n diode, either efficient optical modulation or detection is demonstrated. As an electroabsorption modulator, a fiber-optic link with a -17.4-dB RF loss and a 124-dB-Hz$^{4/5}$ suboctave spurious-free dynamic range is obtained with electrical biases in the 2 to 3 V range. As a waveguide photodetector, a 0.45-A/W fiber coupled responsivity, photocurrents up to 20 mA, and an output second-order intercept of $+34.5$ dBm are achieved at 7-V electrical bias.**

I. Introduction

ANALOG fiber-optic links have been shown to be useful in antenna remoting and active phased-array applications for delivering high-frequency RF signals directly to [1] and from [2] antenna elements with minimal signal attenuation, high-dynamic range, and negligible element crosstalk. As the microwave frequency of operation is increased, phased-array antenna element spacing becomes restrictively small resulting in severe front end space and EMI limitations. Small, multiple-function optoelectronic transceiver components can be useful for mitigating these limitations. High-frequency analog fiber-optic links have been demonstrated using interferometric or electroabsorption (EA) integrated optical modulators fabricated in lithium niobate [3], [4], III–V semiconductors [5], and organic polymers [6]. Among these modulator and material candidates, the III–V semiconductor EA modulator offers the shortest device lengths (approximately 100 μm), the simplest electrode design (lumped electrode), and the most mature device fabrication, processing and packaging approaches. The size advantage is further emphasized if dual-function modulator/detector operation can be obtained resulting in extremely compact transmit/receive front end antenna architectures. The multifunction aspect of the semiconductor waveguide device is the focus of this letter.

Giuliani *et al.* [7], have recently demonstrated a multi-functional amplifier-modulator-detector for digital photonic networks. This two-electrode device acts as a modulator and power amplifier or as a preamplifier and detector. In our current work, a single-electrode waveguide transmitter and receiver (transceiver) for use in either single- or multielement antenna remoting applications is demonstrated. Fundamental for the operation of the transceiver is the Franz–Keldysh effect (FKE). This EA mechanism serves a dual-purpose: 1) to apply modulation with moderate absorption and 2) for photodetection at strong absorption. Previous work [8] has shown the FKE to possess high dynamic range properties in a waveguide modulator with small polarization dependence. The present work shows that efficient RF modulation and detection are obtainable in the same waveguide structure. To our knowledge, this is the first reported single-electrode waveguide device intended for use as both a modulator and a detector in a high-performance analog fiber-optic link.

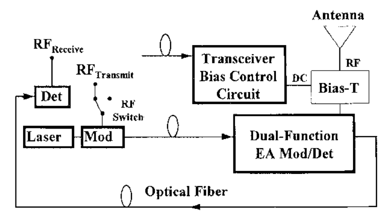

Fig. 1. Schematic of antenna feed network, including optoelectronic transceiver, remote laser, optical detector (Det), and modulator (Mod), used for transmit/receive applications.

The dual-function optoelectronic transceiver has advantage in antenna applications where space is a premium. It eliminates the need for one optoelectronic device at the antenna front end, reducing component and optical fiber count which directly translates into space savings. Further packaging size benefit is obtainable if a reflection mode modulator is used resulting in a single-sided fiber pigtailed device. The reverse biased p-i-n diode transceiver requires an adjustable dc electrical bias to switch from modulator to detector operation. Microwave frequency conversion [9] or other signal processing may be done remotely at the site of the laser source making for a very simple antenna front end architecture. A schematic of a simplified antenna front end including the optoelectronic transceiver is shown in Fig. 1. The waveguide device works as a modulator in receive mode and a detector in transmit mode. The two modes can be remotely switched by control circuitry which can adjust the dc electrical bias with a switching time limited by the associated electronics. The

Manuscript received May 21, 1996; revised July 23, 1996.
R. B. Welstand, J. T. Zhu, and P. K. L. Yu are with the University of California, San Diego, Department of ECE, La Jolla, CA 92093-0407 USA.
S. A. Pappert and C. K. Sun are with NCCOSC RDTE DIV 895, San Diego, CA 92152-5000 USA.
Y. Z. Liu is with the Fermionics Corporation, 4555 Runway Drive, Simi Valley, CA 93063 USA.
Publisher Item Identifier S 1041-1135(96)08154-2.

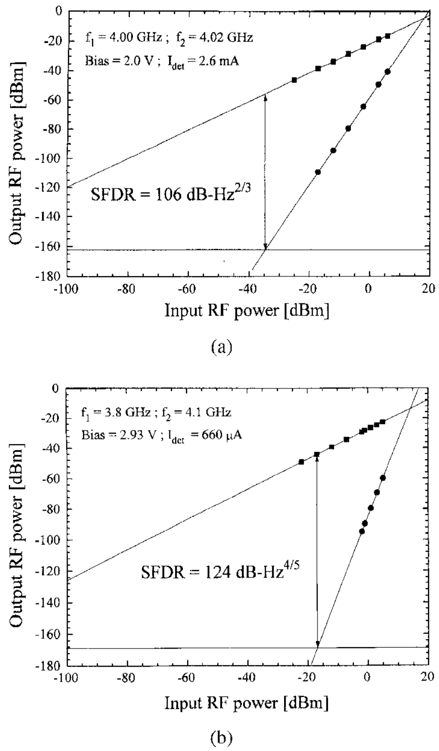

Fig. 2. Two-tone linearity measurement of the transceiver as a waveguide modulator showing fundamental (squares) and third-order intermodulation product (circles) signals. (a) For the broad-band measurement, with 43 mW (TM polarized) light incident onto the device, the extrapolated spurious-free dynamic range at 4 GHz is 106 dB-Hz$^{2/3}$ with 2.6 mA of detector photocurrent, (b) For the narrow-band measurement, with 37 mW (TM polarized) light incident onto the device, the extrapolated spurious-free dynamic range at 4 GHz is 124 dB-Hz$^{4/5}$ with 0.66 mA of detector photocurrent.

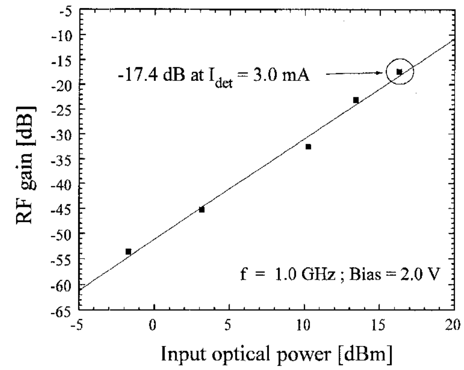

Fig. 3. RF gain at 1 GHz versus input optical power of the transceiver as a waveguide modulator.

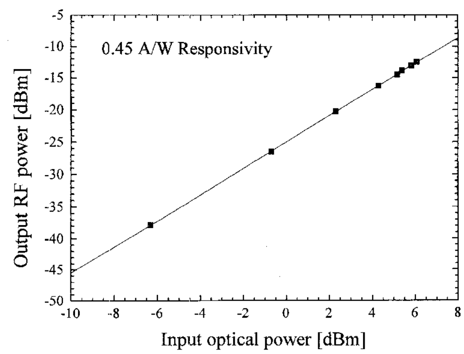

Fig. 4. Detected RF signal power at 4 GHz plotted versus input optical power of the transceiver as a waveguide detector.

modulation and detection characteristics of the semiconductor device are critical to this approach and our results show that little link performance is sacrificed (5 dB added RF link loss due to reduced detector responsivity) in comparison to using a separate optical modulator and a dedicated 0.8 A/W responsivity detector at the antenna site.

II. Experimental

The transceiver structure described herein is the same as reported previously [8]. Briefly, it consists of an undoped InGaAsP ($\lambda = 1.24$ μm) absorbing layer (0.35 μm thick), sandwiched between p- and n- InP layers. An etched mesa of 3 to 5 μm provides lateral light confinement. The waveguides are cleaved to a length of approximately 120 μm. Antireflection coatings are e-beam deposited at the facets to improve the coupling into and out of the waveguide. The measured 3-dB electrical bandwidth for the lumped element device without any matching circuit or termination resistor, is 11 GHz for both modulator and detector operation.

Two experiments are performed to characterize the usefulness of the device in each mode of operation. First, the device is tested as a waveguide modulator, in a fiber link consisting of a high-power 1.32 μm Nd:YAG laser source, an optical polarization controller, the EA modulator, and a surface-illuminated InGaAs p-i-n photodiode (0.77 A/W DC responsivity; 6.5 GHz 3-dB electrical bandwidth). The maximum power incident to the modulator is 43 mW. Two RF tones are supplied to the electrical input through a power combiner, ferroelectric isolators, and a bias-T. Second, the device is tested as a detector, with two temperature-tuned, 1.32 μm Nd:YAG lasers providing the RF signal in a heterodyne configuration. The output of one of the lasers goes into a polarization controller, the output of which is fed into a 3-dB coupler along with the other laser output. One output of the coupler (output power of 4 mW) feeds into a variable attenuator and the waveguide detector. Both modulator and detector responsivity, saturation, and linearity are examined. In the case of the device operating as a waveguide detector, comparison is made to a high speed, surface-illuminated InGaAs photodiode.

III. Waveguide Modulator Performance

The primary concerns for the transceiver as a modulator are large linear dynamic range and high-RF efficiency. These are simultaneously maximized in broad-band or multiple-octave applications by biasing the waveguide device at the maximum slope point on the dc transfer curve, where the second derivative is zero. This null point occurs at 2.0 V for the present device. The broad-band linearity is investigated for the modulator biased at 2.0 V, and results of the two-tone measurement at 4 GHz are shown in Fig. 2(a). For this measurement, the shot-noise-limited detector dc photocurrent is 2.6 mA. The dominant distortion is the third-order intermodulation term. The third-order intercept point (IP3) is -3.6 dBm (output referenced), thus the SFDR extrapolated to the calculated noise floor is 106 dB for a 1-Hz noise bandwidth.

It should be noted that biasing the modulator at the point on the transfer curve where the third derivative is zero, gives a reduction in the third-order intermodulation term [8]. This is desired in high center-frequency, narrow-bandwidth, antenna remoting applications, because the second-order distortions are out of the passband. For the present device, the null bias is 2.93 V with 37 mW incident optical power. Biasing at this null point results in a 0.66 mA dc photocurrent at the detector and a measured SFDR of 124 dB in a 1-Hz noise bandwidth, as shown in Fig. 2(b). The dominant distortion is the third-order intermodulation term, which has a fifth-order power dependence. To maintain the high suboctave and multi-octave SFDR modulator performance over temperature, active modulator bias control is required. Simulation has shown that the modulator bias voltage must be maintained to better than ± 3 mV to incur less than 5-dB SFDR degradation [8].

Fig. 3 shows the measured RF gain at 1 GHz with 6 percent modulation depth versus the input optical power for the modulator biased at 2.0 V, giving the largest RF gain possible for this device. The RF gain of the link shows no saturation up to 43-mW optical power, the largest power available for this measurement. The large power handling capability of this EA modulator enables a substantial RF signal gain, despite the small depths of modulation for spurious signal-free operation. An RF link gain of -17.4 dB with 3.0 mA of dc photocurrent at the detector has been measured representing the largest link gain reported for an EA modulator.

IV. Waveguide Detector Performance

In the detector mode, the transceiver is biased at 7.0 V to assure large absorption. Fig. 4 shows the detected RF signal power at 4 GHz plotted versus input optical power using the two beated lasers. The measurement shows no RF saturation for power levels up to 4 mW, and the measured RF power agrees with values calculated from the measured dc responsivity, $\mathcal{R}$, of 0.45 A/W. Additionally, the dc responsivity is maintained to very large incident optical powers. The maximum photocurrent measured is 20 mA with the maximum incident power from the high-power laser.

The RF output power of a square-law detector is given by

$$1/4 \cdot m^2 \cdot (P_{\mathrm{OPT}})^2 \cdot \mathcal{R}^2 \cdot R_d \tag{1}$$

where m is the modulation depth, R_d is the load impedance (50 Ω) and P_{OPT} is the optical power. In the heterodyned configuration with equal input powers from the two lasers, the modulation depth is one. As can be seen from (1), using a commercially available 11 GHz InGaAs detector [10] with a responsivity of 0.8 A/W gives a larger detected RF power. Therefore, the smaller responsivity of the waveguide detector results in a theoretical RF link gain penalty of 5.0 dB compared to the surface-illuminated InGaAs detector. It is noted that although the RF efficiency of the waveguide device is relatively lower, larger optical powers and frequency bandwidths have been achieved with waveguide photodiodes [11], [12].

The nonlinearity of the waveguide detector is investigated at the second-harmonic frequency of the 4 GHz signal. The second-order intercept point (IP2) is extrapolated to $+34.5$ dBm (output referenced) from the measured second harmonics. The IP3 limits the narrow-band dynamic range of the link the same way as IP2 limits the broad-band dynamic range. Determination of this nonlinear intercept-point is presently limited by the low optical power available from the two beated lasers in our measurement. In the worse case of the third-harmonic power at the measurement noise floor, the extrapolated IP3 would be $+23$ dBm.

V. Conclusion

An InGaAsP–InP waveguide transceiver device is demonstrated as a dual-function modulator and detector. This device has the largest reported link gain of -17.4 dB when used as an EA modulator, and a dc responsivity of 0.45 A/W and output second-order intercept of $+34.5$ dBm when used as a detector. At 4 GHz, the broad-band and narrow-band spurious-free dynamic range of the transceiver as a modulator are, respectively, 106 dB-Hz$^{2/3}$ and 124 dB-Hz$^{4/5}$. The transceiver as a detector handles 20 mA of dc photocurrent, although it suffers an RF link gain penalty of 5.0 dB compared to a high-frequency InGaAs detector.

References

[1] S. T. Chew, D. T. K. Tong, M. C. Wu, and T. Itoh, "Optically assisted microwave active integrated antennas," *IEICE Trans. Electron.*, vol. E79-C, pp. 60–67, 1996.

[2] W. L. Glomb, Jr., "Fiber optic links for antenna remoting," in *Proc. SPIE, Optical Technology for Microwave Applications VI and Optoelectronic Signal Processing for Phased-Array Antennas III*, vol. 1703, 1992, pp. 523–527.

[3] G. E. Betts, C. H. Cox, III, and K. G. Ray, "20 GHz optical analog link using an external modulator," *IEEE Photon. Technol. Lett.*, vol. 2, pp. 923–925, 1990.

[4] G. K. Gopalakrishnan, C. H. Bulmer, W. K. Burns, R. W. McElhanon, and A. S. Greenblatt, "40 GHz low half-wave voltage Ti:$LiNbO_3$ intensity modulator," *Electron. Lett.*, vol. 28, pp. 826–827, 1992.

[5] C. K. Sun, S. A. Pappert, R. B. Welstand, J. T. Zhu, P. K. L. Yu, Y. Z. Liu, and J. M. Chen, "High spurious-free dynamic range fiber link using a semiconductor electroabsorption modulator," *Electron. Lett.*, vol. 31, pp. 902–903, 1995.

[6] C. C. Teng, "Traveling-wave polymeric optical intensity modulator with more than 40 GHz of 3-dB electrical bandwidth," *Appl. Phys. Lett.*, vol. 60, pp. 1538–1540, 1992.

[7] G. Giuliani, P. Cinguino, and V. Seano, "Multifunctional characteristics of 1.5 μm two-section amplifier-modulator-detector SOA," *IEEE Photon. Technol. Lett.*, vol. 8, pp. 367–369, 1996.

[8] R. B. Welstand, C. K. Sun, S. A. Pappert, Y. Z. Liu, J. M. Chen, J. T. Zhu, A. L. Kellner, and P. K. L. Yu, "Enhanced linear dynamic range property of Franz-Keldysh effect waveguide modulator," *IEEE Photon. Technol. Lett.*, vol. 7, pp. 751–753, 1995.

[9] C. K. Sun, R. J. Orazi, and S. A. Pappert, "Efficient microwave frequency conversion using photonic link signal mixing," *IEEE Photon. Technol. Lett.*, vol. 8, pp. 154–156, 1996.

[10] Opto-Technology FD60 high speed InGaAs PIN photodiode spec. sheet, Fermionics, Simi Valley, CA.

[11] A. R. Williams, A. L. Kellner, and P. K. L. Yu, "Saturation measurements of an InGaAs/InP waveguide photodetector," *Electron. Lett.*, vol. 29, pp. 1298–1299, 1993.

[12] K. S. Giboney, R. L. Nagarajan, T. E. Reynolds, S. T. Allen, R. P. Mirin, M. J. W. Rodwell, and J. E. Bowers, "Traveling-wave photodetectors with 172 GHz bandwidth and 76 GHz bandwidth-efficiency product," *IEEE Photon. Technol. Lett.*, vol. 7, pp. 412–414, 1995.